FOLIA HISTOCHEMICA ET CYTOBIOLOGICA
Vol. 61, No. 1, 2023
pp. 47–55

ORIGINAL PAPER

VIA MEDICA

Focused ultrasound restrains the growth of orthotopic colon cancer *via* promoting pyroptosis

Weixing Mo[1]*, Qingqing Yu[2]*, Xiufeng Kuang[3], Ting He[4], Jun Lou[5], Rongjun Tang[2], Ke Zhang[2], Lingdi Li[6], Linfang Zhao[7]

[1]Department of Radiology, Affiliated Hangzhou Cancer Hospital, Zhejiang University School of Medicine, Hangzhou, China

[2]Hyperthermia Center, Affiliated Hangzhou Cancer Hospital, Zhejiang University School of Medicine, Hangzhou, China

[3]Department of Ultrasonography, First People's Hospital of Linping District, Hangzhou, China

[4]Department of Ultrasonography, Affiliated Hangzhou First People's Hospital, Zhejiang University School of Medicine, Hangzhou, China

[5]Department of Ultrasonography, Affiliated Hangzhou Cancer Hospital, Zhejiang University School of Medicine, Hangzhou, China

[6]Department of Medical Oncology, Affiliated Hangzhou Cancer Hospital, Zhejiang University School of Medicine, Hangzhou, China

[7]Department of Ultrasonography, The Third Affiliated Hospital of Zhejiang University of Traditional Chinese Medicine, Hangzhou, China

* Weixing Mo and Qingqing Yu contributed to this work equally.

Abstract

Introduction. Focused ultrasound (FUS) is a non-invasive tumor therapy technology emerging in recent years, which can treat various solid tumors. However, it is unclear whether FUS can affect the pyroptosis of colon cancer (CC) cells. Here, we analyzed the effect of FUS on pyroptosis in the orthotopic CC model.

Material and methods. After an orthotopic CC mouse model was constructed by injecting CT26-Luc cells, BABL/C mice were allocated to the normal, tumor, FUS, and FUS + BAY11-7082 (pyroptosis inhibitor) groups. We monitored the tumor status of the mice through *in vivo* fluorescence image analysis. The histopathological injury of the intestinal tissue and the expression of IL-1β, IL-18, caspase-recruitment domain (ASC), cleaved caspase-1, gasdermin D (GSDMD), and NLRP3 of the CC tumors were examined utilizing hematoxylin and eosin staining, immunohistochemical assay, and Western blot.

Results. FUS restrained the fluorescence intensity of the tumors in orthotopic CC mice, while FUS-mediated suppression of the bioluminescent signal of the tumors was alleviated by BAY11-7082. FUS was found to relieve the injury of the intestinal tissues in CC mice as revealed by morphology. Furthermore, the expressions of IL-1β, IL-18, GSDMD, ASC, cleaved caspase-1, and NLRP3 of the CC tumors in the FUS group were higher than those in the tumor group,

Correspondence addresses:
Linfang Zhao
Department of Ultrasonography, The Third Affiliated Hospital of Zhejiang University of Traditional Chinese Medicine, Hangzhou, China
e-mail: tigeryeah2022@163.com

Lingdi Li
Department of Medical Oncology, Affiliated Hangzhou Cancer Hospital, Zhejiang University School of Medicine, Hangzhou, China
e-mail: lilingdi2002413@126.com

Folia Histochem Cytobiol. 2023
10.5603/FHC.a2023.0003
ISSN 0239-8508, e-ISSN 1897-5631

www.journals.viamedica.pl/folia_histochemica_cytobiologica

while BAY11-7082 addition partly reversed the FUS's effects on orthotopic CC model mice.
Conclusions. Our results pointed out that FUS presented anti-tumor activity in experimental CC, and its mechanism was correlated with the promotion of pyroptosis.

Keywords: CT26-Luc cells; orthotopic colon cancer; focused ultrasound; pyroptosis; gasdermin D; NLRP3

Introduction

Colon cancer (CC) is a digestive system disease that seriously threatens human health [1]. With the change in people's lifestyle and eating habits, the morbidity and mortality of CC are increasing year by year [2]. In 2021, the number of new CC cases ranked third among all tumors, accounting for 8% of global cancer deaths [3]. It has been reported that only about 35% of CC patients are caused by genetic factors, while most cases are caused by a variety of external factors such as a high-fat diet, alcohol consumption, and smoking [4]. CC patients have no evident clinical symptoms in the early stage, and patients in the middle and late stages have abdominal pain, abdominal distention, dyspepsia, and abnormal defecation, while patients in the late stages have distant metastasis and organ dysfunction with poor prognosis [5, 6]. The key to the treatment of CC is early detection and diagnosis, and surgical resection is still the most effective method at present [7]. Yet, most patients have reached the advanced stage before being diagnosed with CC and have lost the chance for surgical treatment [8]. In addition, despite some advances in surgery, chemotherapy, radiotherapy and targeted therapies, toxicity and side effects of radiotherapy and chemotherapy, drug resistance and safety of targeted drugs have not been addressed [9]. Therefore, it is urgent problem to seek a more safe and more effective method with fewer side effects.

Focused ultrasound (FUS) is an emerging technology for tumor local ablation; this non-invasive, safe, and reliable local ablation therapy has been extensively applied in clinical practice [10]. The principle of FUS is that ultrasound can penetrate the physical properties of soft tissue and cause coagulation necrosis of the target tissue [11]. Numerous reports described that FUS can be employed for the treatment of benign and malignant tumors of the liver, colon, breast, kidney, pancreas, and brain [12]. FUS has been reported to induce the expressions of pro-inflammatory cytokines (IL-12, IFN-γ, and TNF-α) after treatment in a variety of cancer cell lines and *in vivo* tumors [13, 14]. Among them, one of the considerable reasons for the aggravation of the inflammatory response is the occurrence of pyroptosis; pyroptosis can not only cause local inflammation, but also lead to the gradual amplification of the inflammatory response [15]. Therefore, the effect of FUS on pyroptosis in CC is what this study wants to explore.

Pyroptosis is a programmed cell death accompanied by an inflammatory response, which is characterized by continuous cell distension until the cell membrane ruptures, leading to the release of cellular contents and activating a strong inflammatory response, thus inducing inflammatory necrosis [16]. Except for the inflammatory signaling pathway such as NLRP3, pyroptosis is also mediated by the gasdermin family, including gasdermin D (GSDMD), which could be cleaved by caspase-1 to trigger pyroptosis [16, 17]. Pyroptosis was extensively related to the initiation and development of multiple diseases such as viruses, bacteria, fungal infection, arteriosclerosis, and cancer [18, 19]. Since the occurrence of pyroptosis may affect every stage of tumor formation, it has become a new hot spot in tumor research [20]. According to related studies, pyroptosis-related factors were associated with tumors; for example, the deletion of the caspase-1 gene led to colitis-related colon cancer; IL-1β secreted by melanoma could notably enhance the synthesis of IL-1 in melanoma cells and mediate macrophage recruitment and angiogenesis *in vitro* [21, 22]. In addition, caspase-1 can mediate the production of IL-18, which is further involved in the pyroptosis [22]. However, there are few reports on the effect of FUS ablation on pyroptosis.

Therefore, CT26-Luc cells were exploited to establish a visual orthotopic CC mouse model. After FUS ablation treatment, the effect of this treatment on the pyroptosis of orthotopic CC tumor cells was analyzed. This experiment was designed to clarify the mechanism of FUS in the treatment of orthotopic CC lesions.

Materials and methods

Animals. Shanghai Jihui Animal Laboratory Co. Ltd. provided 40 male BABL/C mice (7 weeks old). All mice were adaptively fed for 7 days in a breeding room (25 ± 2° temperature and 55 ± 5% humidity) with 12 hours of circulating light.

Cell lines. Mouse CC cell line expressing luciferase, CT26-Luc cell line (iCell-m014), was acquired from iCell Bioscience (China). For the culture of CT26-Luc cells, RPMI-1640 complete medium (M0201A, WHELAB, China) was applied. CT26-Luc cells were put in a cell incubator (BB150, Thermo Fisher, USA) at 37° with 5% CO_2. Cells in the logarithmic phase were used for the establishment of the orthotopic CC model.

Animal model of a visual orthotopic CC. Forty BABL/C mice were randomly assigned into the normal group, tumor group, FUS group, and FUS + BAY11-7082 group, with 10 mice in

each group. The visual orthotopic CC model was carried out as follows [23]: to deeply anesthetize all mice, they were placed in an airtight chamber with 3% isoflurane (792632, Sigma-Aldrich, St. Louis, MO, USA). Anesthesia was kept *via* spontaneous respiration of 2% isoflurane. After each mouse was fixed in a supine position and the abdominal skin was sterilized, we used ophthalmic scissors to cut the abdominal cavity longitudinally near the colon to expose the colon and find the descending colon. Next, we used an insulin needle to inject CT26-Luc cell suspension (0.5 mL, 1×10^7/mL) under the intestinal membrane and gently glued the injection needle orifice with an appropriate amount of cosmetic glue. Then, the exposed colon was carefully placed back into the abdominal cavity, and the mouse abdomen was sutured with degradable surgical sutures. Mice in the control group were injected with an equal volume of normal saline at the same site. After 7 days of modeling, some mice in the model group and the normal group were dissected, and photographs of the tumor and colon were made.

Seven days after modeling, mice in the FUS group and FUS + BAY11-7082 group were treated with local FUS after anesthesia and fixation. A FUS transducer (V3330) was provided by Olympus (Houston, TX, USA). The irradiation intensity was 9.3 MHz and the power was 4.5 W. FUS treatment started from the center of the tumor and gradually expanded to the edges with a point spacing of 1.0 mm. The exposure time at each treatment point was 10 s [24]. Except for the FUS treatment according to the described procedure, mice in the FUS + BAY11-7082 group were also injected intratumorally with 5 mg/kg of BAY11-7082 (B5556, Sigma-Aldrich) under the guidance of ultrasound after modeling, on days 1 and 4 after initiating FUS treatment.

***In vivo* fluorescence image analysis.** After seven days of treatment, 100 μL of 1 mg/mL D-luciferase (E1601, Promega, Madison, WI, USA) in 0.9% NaCl was injected intraperitoneally. After 5 min, a small animal *in vivo* fluorescence image analysis system (IVIS Spectrum, Caliper, USA) was employed to monitor the tumor status of each mouse.

Collection of samples. After *in vivo* fluorescence image analysis, each mouse was euthanized through inhalation of CO_2. The CC tumors were dissected for hematoxylin and eosin (H&E) and immunohistochemical (IHC) stainings, and Western blot assay.

H&E staining. Part of the mice intestinal tissue in each group was fixed in 10% neutral formalin buffered solution (F301880, Aladdin, Shanghai, China) for one day. Then specimens were dehydrated and embedded in paraffin. The serial sections (10 μm) were acquired utilizing a pathologic microtome (RM2016, Leica, Beijing, China). Next, the dewaxed and hydrated sections were stained with hematoxylin (G1004, Servicebio, Wuhan, China) for 5 min. After being differentiated with 1% hydrochloric acid, the sections were treated with 1% eosin solution (C0109, Beyotime, Shanghai, China) for 120 s. After dehydration and transparency checking, neutral balsam (36313ES60, Yeasen, Shanghai, China) was selected to seal the sections. The tissue integrity was monitored with a microscope (BX53M, Olympus, Tokyo, Japan) at the magnification of 200× and 400×.

Immunohistochemistry. The antigen retrieval was done on the dewaxed and hydrated tumor sections with citric acid antigen repair solution (Servicebio, pH 6.0) at 95–99ºC, 10 min. To inactivate endogenous catalase, 3% H_2O_2 was chosen to treat the sections for 8 min. For the blocking of sections, 5% BSA Blocking Buffer was applied. Further incubation was carried out by adding primary rabbit anti-mouse antibodies against GSDMD (1:200, AF4013, Affinity, USA), IL-18 (1:200, DF6252, Affinity), and IL-1β (1:200, AF5103, Affinity) at 4° all night. The secondary antibody goat anti-rabbit IgG H&L (HRP) (1:1000, ab6721, Abcam, Cambridge, UK) was then applied to treat the sections (37°, 60 min). For visualization of the sections, DAB (abs9210, Absin, China) was utilized. After counterstaining nuclei with hematoxylin, slides were analyzed by microscopy at the magnifications of 200× and 400×. The GSDMD, IL-1β and IL-18 immunoreactivity was visualized in brown, while nuclei stained with blue. The relative expression of GSDMD, IL-1β, and IL-18 was semiquantitatively analyzed by ImageJ software (NIH, Bethesda, MD, USA) based on the ratio of the brown-stained area/total area of the section.

Western blot. We applied RIPA buffer (PC104, Epizyme, China) to extract proteins from the CC tumors. For quantification of the lysed protein, a BCA protein kit (BI-WB005, SBJBIO, China) was applied. After denaturation and electrophoresis, they were blotted onto the nitrocellulose membrane and blocked in 5% BSA. After that, the blocked membrane was immersed in the solution of primary antibodies (4°, overnight) and on the next day with secondary antibody (1:10000) at 37° for 60 min. After visualizing with ECL reagent (GK10008, GlpBio, Montclair, CA, USA), the gel was analyzed with an Imaging System (Geliance 200, PerkinElmer, Waltham, MA, USA). The primary antibodies against GSDMD (1:2000, AF4013), IL-18 (1:2000, DF6252), IL-1β (1:2000, AF5103), ASC (1:2000, DF6304), cleaved-Caspase 1 (1:1000, AF7022), NLRP3 (1:2000, DF7438), and β-actin (1:20000, AF7018) were from Affinity (Milwaukee, WI, USA).

Statistics. For analysis of statistics, SPSS software (version 16.0, IBM, Armonk, NY, USA) was selected. Data in three independent experiments were displayed as mean ± standard deviation. One-way ANOVA was applied for comparing the differences among multiple groups, and pairwise comparison between groups was estimated by the Tukey test. The Kruskal--Wallis H test was utilized to those with uneven variance. The statistical significance was defined as $P < 0.05$.

Results

The combined FUS and BAY11-7082 restrained the fluorescence intensity of the tumors in orthotopic CC mice

Compared to the colon of the normal group, more tumor nodes could be found in the colon of mice in the tumor group, which preliminarily demonstrated that we have established an orthotopic CC mouse

Folia Histochem Cytobiol. 2023
10.5603/FHC.a2023.0003
ISSN 0239-8508, e-ISSN 1897-5631

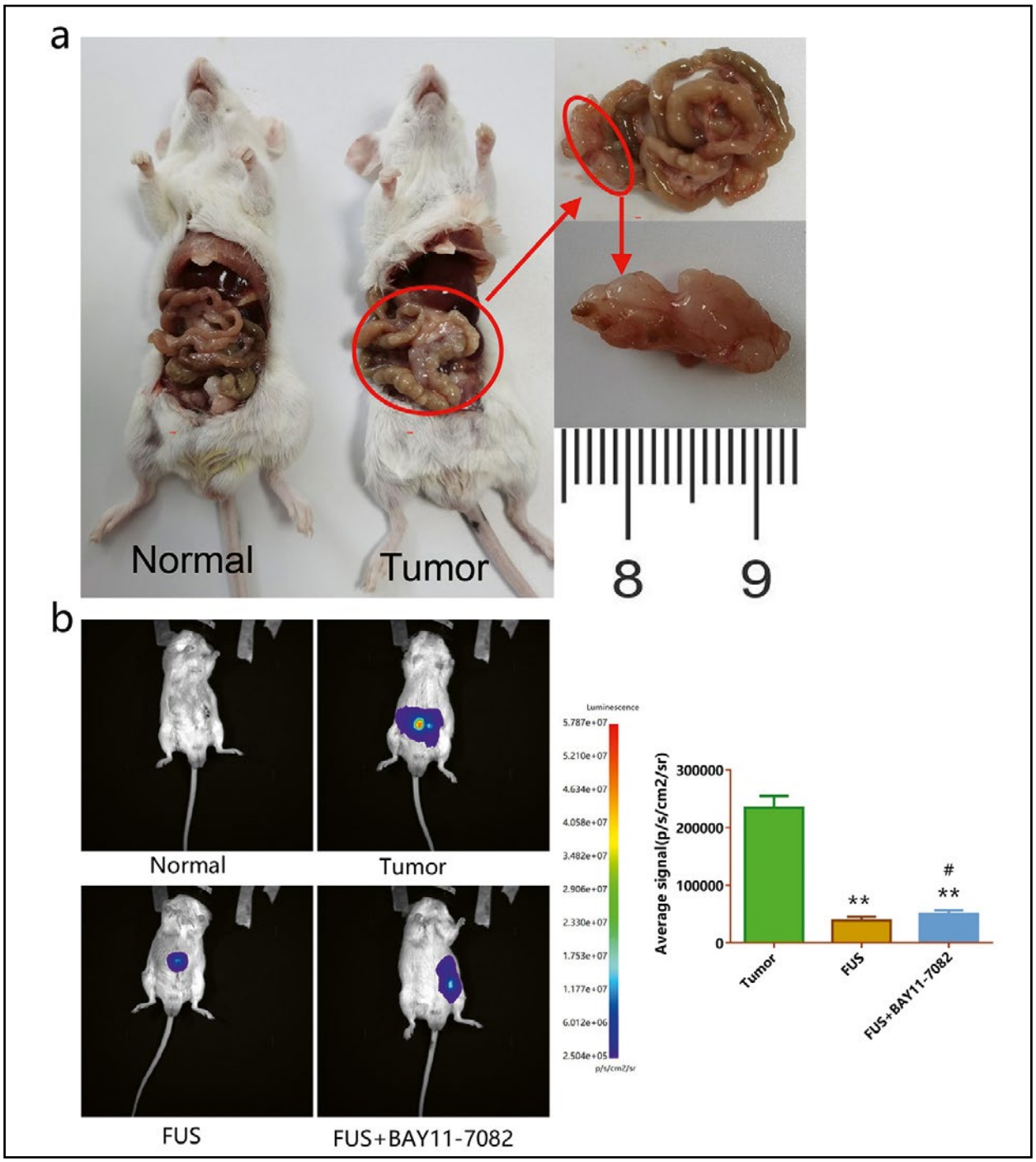

Figure 1. The combined administration of FUS and BAY11-7082 restrained the fluorescence intensity of the tumors in orthotopic colon cancer (CC) model mice. **A.** Establishment of an orthotopic CC mouse model. **B.** Small animal *in vivo* fluorescence image analysis system was applied to assess the fluorescence intensity of the tumors in orthotopic CC mice. Quantitative data were displayed as mean ± SD, n = 5. $^{**}P < 0.01$ *vs.* tumor group; $^{\#}P < 0.05$ *vs.* FUS group. Abbreviations: FUS — focused ultrasound; CC — colon cancer.

model successfully (Fig. 1a). Subsequently, *in vivo* fluorescence image analysis presented that FUS alone or co-treatment of FUS and BAY11-7082 alleviated the fluorescence intensity of the tumors in CC model mice (Fig. 1b, $P < 0.01$). Relative to the FUS group, the fluorescence intensity of the tumors in the FUS + BAY11-7082 group was higher (Fig. 1b, $P < 0.05$).

BAY11-7082 reversed the alleviation effect of FUS on intestinal injury in CC mice

H&E staining was used to observe the histological damage of each group in CC mice intestinal tissues. As displayed in Fig. 2 the tumor lesion of the colonic tissues in the tumor group presented obvious inflammatory cell aggregation and tumor cells encapsulated

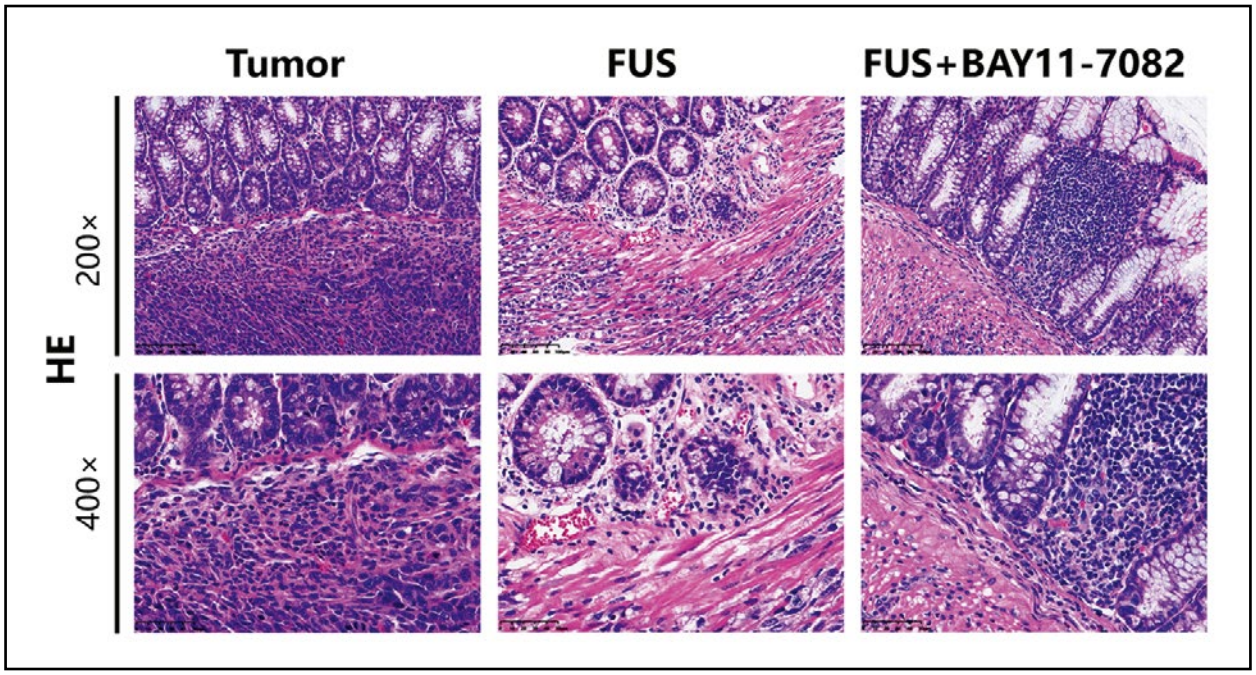

Figure 2. FUS suppressed the histopathological injury of colon tissue in the orthotopic colon cancer (CC) model mice, while BAY11-7082 offset this effect. The representative microphotographs (magnifications: 200×, scale bar = 100 μm; 400×, scale bar = 50 μm) of hematoxylin-eosin stained CC tumors were presented.

intestinal tissue. Compared with the tumor group, the tumor lesion of mice in the FUS group had fewer inflammatory cell aggregation and a lower number of tumor cells, the intestinal tissue structure was relatively complete and the degree of damage was low. However, the addition of BAY11-7082 in FUS group caused the alleviation effect of FUS on intestinal damage and tumor morphology was partly offset.

BAY11-7082 reversed the facilitation of FUS on the expressions of GSDMD, IL-1β, and IL-18 of the tumors in CC mice

The immunoreactivity of GSDMD, IL-1β, and IL-18 in the CC tumors was analyzed by IHC staining. The immunoexpressions of GSDMD, IL-1β, and IL-18 of the CC tumors in the FUS group and the FUS + BAY11-7082 group were higher than those in the tumor group (Fig. 3a–c, $P < 0.01$). Furthermore, we found that BAY11-7082 administration partially suppressed the stimulatory effect of FUS on the expression of the above-mentioned pyroptosis-related markers in the CC tumors (Fig. 3a–c, $P < 0.05$).

BAY11-7082 counteracted the up-regulation of FUS on pyroptosis-related markers of the CC tumors

The expression of pyroptosis-related markers was examined by Western blotting (Fig. 4a, b). As can be seen, the protein levels of IL-1β, ASC, cleaved caspase-1, and NLRP3 of the CC tumors in the FUS group were higher relative to the tumor group; FUS also largely increased the protein expressions of IL-18 and GSDMD of the CC tumors (Fig. 4a, b, $P < 0.05$). In addition, FUS-induced up-regulation of the levels of these pyroptosis-related markers was partly reversed by BAY11-7082 addition (Fig. 4a, b, $P < 0.05$).

Discussion

Orthotopic transplantation is used to study the tumorigenic characteristics and metastatic capacity of cancer by transplanting tumors into the same organ or other recipient animals [25]. To better simulate the CC tumor growth characteristics, in this study, an orthotopic CC mouse model was constructed by injection CT26-Luc cells into the colon wall of BABL/C mice. Previous studies proved that the pathological changes of normal and malignant human tissues exposed to FUS exhibited coagulative necrosis and severe damage to the microvascular system in the thermal ablation CC tumors [26]. In our research, to check the impact of FUS on tumor formation in orthotopic CC mice, we first monitored the small animal *in vivo* fluorescence images and found that FUS alone or co-treatment with BAY11-7082 reduced the growth and bioluminescence signals of orthotopically transplanted CC cells (CT-26-Luc cells). However, the BAY11-7082 slightly, although significantly, reduced the repressive effect

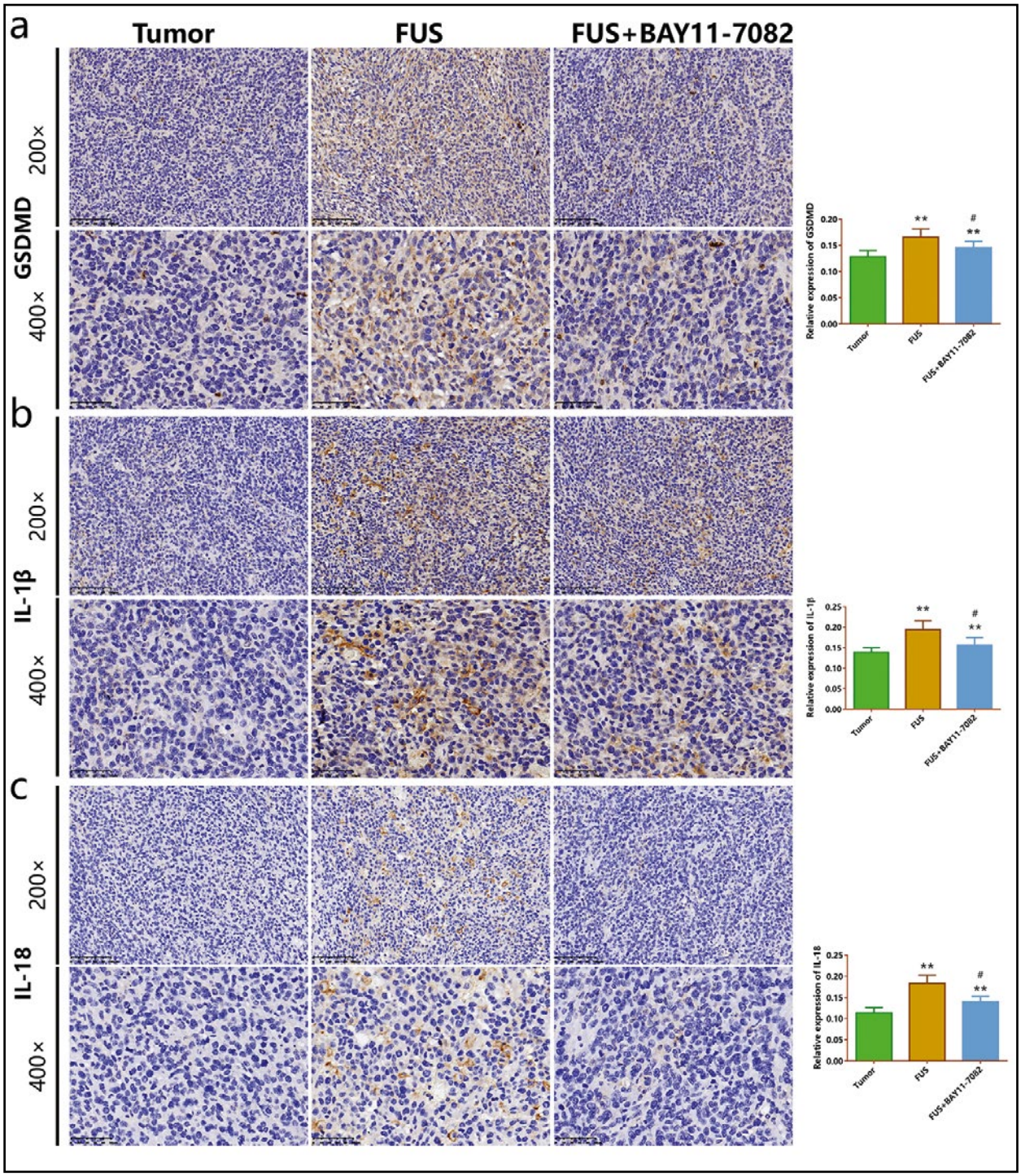

Figure 3. BAY11-7082 partially reversed the FUS-induced tissue immunoreactivity of GSDMD, IL-1β, and IL-18 in the tumors of orthotopic CC model mice. **A–C.** The expression of GSDMD, IL-1β, and IL-18 of the CC tumors in each group were examined by immunohistochemical assay (magnifications: 200×, scale bar = 100 μm; 400×, scale bar = 50 μm). The relative expression of GSDMD, IL-1β and IL-18 were presented as mean ± SD, n = 6. $^{**}P < 0.01$ *vs.* tumor group; $^{\#}P < 0.05$ *vs.* FUS group. Abbreviations: GSDMD — gasdermin D; IL-18 — interleukin-18; IL-1β, — interleukin-1β.

of FUS on the bioluminescence signals of orthotopic CC. FUS could focus ultrasonic energy on tumor tissue, and cause coagulative necrosis of tumor cells through thermal effect [27]. Lee *et al*. revealed that in this way FUS might exert its anti-tumor effect in rats by destroying cervical cancer tumor cells and inducing tumor cell necrosis [28]. The HE staining confirmed that FUS could induce morphological damage to and accelerate the necrosis of the CC tumor cells, alleviate the intestinal injury; while BAY11-7082 partly offset

Folia Histochem Cytobiol. 2023
10.5603/FHC.a2023.0003
ISSN 0239-8508, e-ISSN 1897-5631

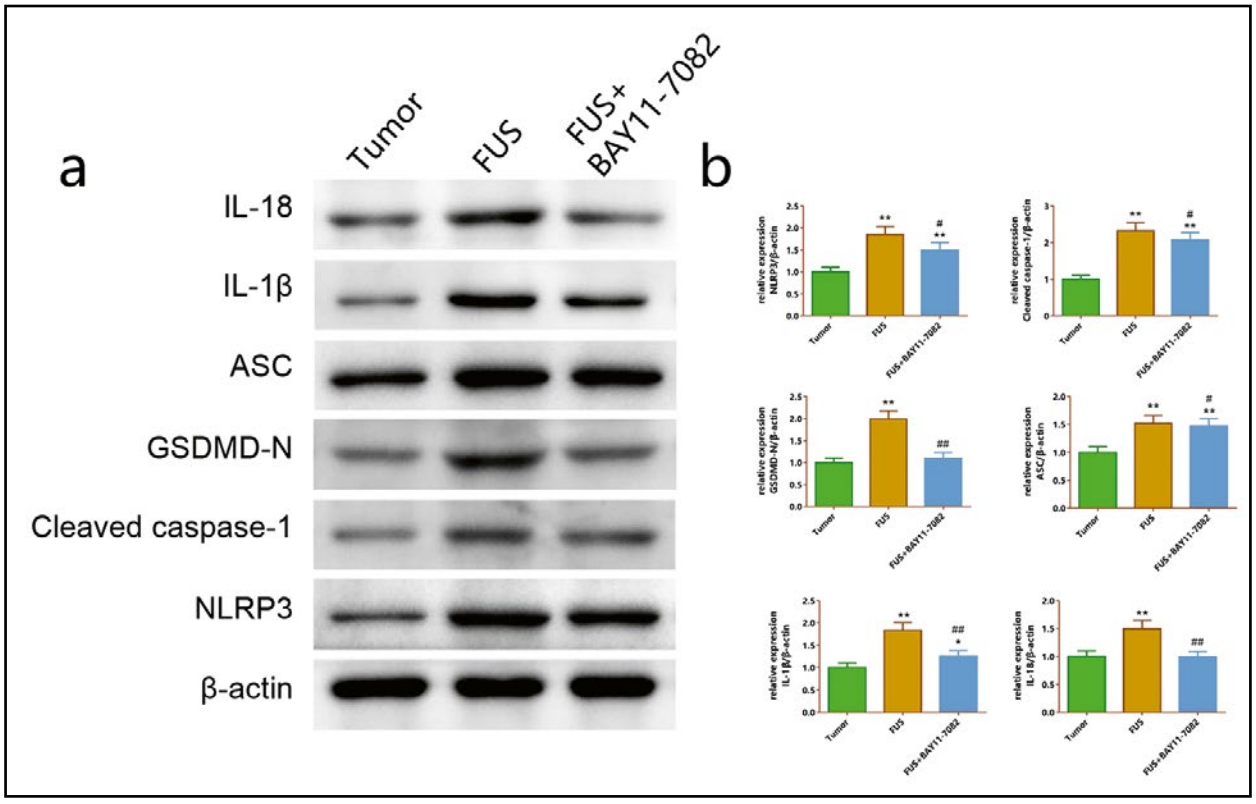

Figure 4. BAY11-7082 partially counteracted the up-regulation of FUS-induced immunoexpression of pyroptosis-related markers in the tumors of orthotopic CC model mice. **A.** The representative Western blots of pyroptosis-associated proteins. **B.** The levels of IL-1β, IL-18, ASC, GSDMD, cleaved caspase-1, and NLRP3 in the CC tumors were measured semiquantitatively by Western blotting. Data were presented as mean ± SD, n = 3. $^{*}P < 0.05$, $^{**}P < 0.01$ *vs.* tumor group; $^{\#}P < 0.05$, $^{\#\#}P < 0.01$ *vs.* FUS group. Abbreviations: ASC — apoptosis-associated speck-like protein containing CARD; NLRP3 — NOD-like receptor thermal protein domain associated protein 3.

the ameliorative effect of FUS on intestinal damage in orthotopic CC model mice. All these directly confirmed that FUS could effectively restrain the growth of the tumors in CC rats.

Thermal ablation of tumors can destroy tumor cells *in vivo* and induce inflammatory responses in the body, while inflammation manifests a considerable role in various stages of tumor development, including initiation, progression, and metastasis [29]. Researchers also point out that the thermal ablation of tumors is a kind of trauma inside the body, which can induce the release of pro-inflammatory cytokines from the ablated tissue or tumor cells [30]. In a single-center study of patients with abdominal tumors, an early post-ablation inflammatory response with a significant increase of leukocytes, CRP, IL-6 within the first 20 h after FUS was observed, accompanied by significant reduction of tumor size during one-year follow-up [31]. In addition, FUS can induce acute inflammatory responses, activate immune cells, destroy CC tumors, and can be used in combination with other treatments to enhance efficacy [32, 33]. By conducting IHC assay and Western blot analysis, our results proved that FUS was able to induce the expression of inflammatory factors in the tumors of orthotopic CC mice. As mentioned above, FUS ablation therapy can lead to tumor cell death and secretion of inflammatory factors, which are often accompanied by pyroptosis. Therefore, we next explored the effects of FUS on pyroptosis in orthotopic CC.

It has been reported that excessive activation of pyroptosis can cause abundant inflammatory responses and involve the initiation and development of tumors [34]. Gasdermin can be cleaved by caspase-1 activated by inflammasomes and caspase-4, caspase-5 and, caspase-11 activated by other pathways [35]. Gasdermin-N binds to cell membrane lipids, causing cells to swell and rupture, and release pro-inflammatory factors such as IL-1β and IL-18 [36]. NLRP1, NLRP3, NLRC4, ASC, and pro-caspase-1 bind to form inflammasome when stimulated by pathogen damage-related molecular patterns [37]. The study using NLRP3 or caspase-1 knockout mice demonstrated that mice lacking inflammasome activation are more prone to CC than control animals [38]. It was confirmed that prostate tumors treated with FUS presented milder and more chronic inflammation within 180 days after FUS treatment as compared with before FUS treatment

Folia Histochem Cytobiol. 2023
10.5603/FHC.a2023.0003
ISSN 0239-8508, e-ISSN 1897-5631

[39]. In our study, after co-treatment with FUS and BAY11-7082, pyroptosis-related markers in the CC tumors showed a trend of high expression, and the activation effect of FUS on pyroptosis-related factors was partially reversed by BAY11-7082. The above results revealed that FUS weakened the growth of orthotopic CC tumors by promoting pyroptosis.

As a non-invasive method, reports showed that the main mechanisms of FUS ablation involve mechanical and thermal effects. The thermal effect of FUS can cause tumor cell degeneration necrosis or solidification necrosis [40]. In addition, tumor cells undergo a series of functional and structural changes under mechanical effects, such as increased cell membrane permeability, organelle damage, and cell nucleus fragmentation [41]. These effects can destroy and embolize small arteries, capillaries and small veins, effectively inhibit tumor regeneration and metastasis, and also can cause cell destruction and death [42]. Furthermore, both mechanical and thermal effects of FUS can initiate immune responses in tumors by releasing tumor-associated antigens that lead to the activation of the immune cells in the tumor microenvironment, such as tumor-infiltrating lymphocytes, dendritic cells and macrophages [43]. Among these, cell pyroptosis is a part of the anti-tumor mechanism, which can lead to tumor cell death. Therefore, the addition of pyroptosis inhibitor cannot offset the anti-tumor effect of FUS totally. This research is a preliminary study to investigate the effect and potential mechanism of FUS in colon cancer. In further studies, more possible mechanisms need to be explored to explain the anti-tumor effect of FUS.

This study successfully established an orthotopic CC tumor model of CT26-Luc BABL/C mouse. It was found that FUS effectively repressed tumor growth in orthotopic CC mice, and its mechanism was related to the promotion of pyroptosis. Our study provides significant insights into the exact mechanism of FUS action in the treatment of CC.

Ethics statement

All procedures involving animals conformed to the protocols stipulated by Zhejiang Eyong Pharmaceutical Research and Development Center (SYXK(Zhe)2021-0033) and based on the guidelines of the Institutional Animal Care and Use Committee.

Conflict of interests

All authors declare there are no competing interests.

Authors' contributions

Weixing Mo and Linfang Zhao designed the study; Weixing Mo, Qingqing Yu, Jun Lou, Rongjun Tang, and Ke Zhang performed experiments, and analyzed the data; Weixing Mo, Qingqing Yu, and Lingdi Li wrote the manuscript; Linfang Zhao and Lingdi Li revised the manuscript. All authors approved the submission.

References

1. Yamazaki K, Matsumoto S, Imamura CK, et al. Clinical impact of baseline renal function on safety and early discontinuation of adjuvant capecitabine plus oxaliplatin in elderly patients with resected colon cancer: a multicenter post-marketing surveillance study. Jpn J Clin Oncol. 2020; 50(2): 122–128, doi: 10.1093/jjco/hyz149, indexed in Pubmed: 31665356.
2. Siegel RL, Miller KD, Goding Sauer A, et al. Colorectal cancer statistics, 2020. CA Cancer J Clin. 2020; 70(3): 145–164, doi: 10.3322/caac.21601, indexed in Pubmed: 32133645.
3. Siegel RL, Miller KD, Fuchs HE, et al. Cancer Statistics, 2021. CA Cancer J Clin. 2021; 71(1): 7–33, doi: 10.3322/caac.21654, indexed in Pubmed: 33433946.
4. Torre LA, Bray F, Siegel RL, et al. Global cancer statistics, 2012. CA Cancer J Clin. 2015; 65(2): 87–108, doi: 10.3322/caac.21262, indexed in Pubmed: 25651787.
5. Otani K, Kawai K, Hata K, et al. Colon cancer with perforation. Surg Today. 2019; 49(1): 15–20, doi: 10.1007/s00595-018-1661-8, indexed in Pubmed: 29691659.
6. Jahanafrooz Z, Mosafer J, Akbari M, et al. Colon cancer therapy by focusing on colon cancer stem cells and their tumor microenvironment. J Cell Physiol. 2020; 235(5): 4153–4166, doi: 10.1002/jcp.29337, indexed in Pubmed: 31647128.
7. Wang YN, Chen ZH, Chen WC. Novel circulating microRNAs expression profile in colon cancer: a pilot study. Eur J Med Res. 2017; 22(1): 51, doi: 10.1186/s40001-017-0294-5, indexed in Pubmed: 29187262.
8. Takahashi H, Takahashi M, Ohnuma S, et al. microRNA-193a-3p is specifically down-regulated and acts as a tumor suppressor in BRAF-mutated colorectal cancer. BMC Cancer. 2017; 17(1): 723, doi: 10.1186/s12885-017-3739-x, indexed in Pubmed: 29115941.
9. Gurba A, Taciak P, Sacharczuk M, et al. Gold (III) Derivatives in Colon Cancer Treatment. Int J Mol Sci. 2022; 23(2), doi: 10.3390/ijms23020724, indexed in Pubmed: 35054907.
10. Marinova M, Huxold HC, Henseler J, et al. Clinical effectiveness and potential survival benefit of us-guided high-intensity focused ultrasound therapy in patients with advanced-stage pancreatic cancer. Ultraschall Med. 2019; 40(5): 625–637, doi: 10.1055/a-0591-3386, indexed in Pubmed: 29665583.
11. Colen RR, Sahnoune I, Weinberg JS. Neurosurgical applications of high-intensity focused ultrasound with magnetic resonance thermometry. Neurosurg Clin N Am. 2017; 28(4): 559–567, doi: 10.1016/j.nec.2017.05.008, indexed in Pubmed: 28917284.
12. Maloney E, Hwang JHa. Emerging HIFU applications in cancer therapy. Int J Hyperthermia. 2015; 31(3): 302–309, doi: 10.3109/02656736.2014.969789, indexed in Pubmed: 25367011.
13. Wu F, Wang ZB, Cao YD, et al. Expression of tumor antigens and heat-shock protein 70 in breast cancer cells after high-intensity focused ultrasound ablation. Ann Surg Oncol. 2007; 14(3): 1237–1242, doi: 10.1245/s10434-006-9275-6, indexed in Pubmed: 17187168.
14. Hu Z, Yang XYi, Liu Y, et al. Release of endogenous danger signals from HIFU-treated tumor cells and their stimulatory ef-

fects on APCs. Biochem Biophys Res Commun. 2005; 335(1): 124–131, doi: 10.1016/j.bbrc.2005.07.071, indexed in Pubmed: 16055092.
15. Wang Q, Wu J, Zeng Y, et al. Pyroptosis: A pro-inflammatory type of cell death in cardiovascular disease. Clin Chim Acta. 2020; 510: 62–72, doi: 10.1016/j.cca.2020.06.044, indexed in Pubmed: 32622968.
16. Shi J, Gao W, Shao F. Pyroptosis: gasdermin-mediated programmed necrotic cell death. Trends Biochem Sci. 2017; 42(4): 245–254, doi: 10.1016/j.tibs.2016.10.004, indexed in Pubmed: 27932073.
17. Burdette BE, Esparza AN, Zhu H, et al. Gasdermin D in pyroptosis. Acta Pharm Sin B. 2021; 11(9): 2768–2782, doi: 10.1016/j.apsb.2021.02.006, indexed in Pubmed: 34589396.
18. Chen L, Weng B, Li H, et al. A thiopyran derivative with low murine toxicity with therapeutic potential on lung cancer acting through a NF-κB mediated apoptosis-to-pyroptosis switch. Apoptosis. 2019; 24(1-2): 74–82, doi: 10.1007/s10495-018-1499-y, indexed in Pubmed: 30519834.
19. Jiao Y, Zhao H, Chen G, et al. Pyroptosis of MCF7 cells induced by the secreted factors of hUCMSCs. Stem Cells Int. 2018; 2018: 5912194, doi: 10.1155/2018/5912194, indexed in Pubmed: 30534157.
20. Wang YY, Liu XL, Zhao R. Induction of pyroptosis and its implications in cancer management. Front Oncol. 2019; 9: 971, doi: 10.3389/fonc.2019.00971, indexed in Pubmed: 31616642.
21. Shi J, Zhao Y, Wang K, et al. Cleavage of GSDMD by inflammatory caspases determines pyroptotic cell death. Nature. 2015; 526(7575): 660–665, doi: 10.1038/nature15514, indexed in Pubmed: 26375003.
22. Dunn JH, Ellis LZ, Fujita M. Inflammasomes as molecular mediators of inflammation and cancer: potential role in melanoma. Cancer Lett. 2012; 314(1): 24–33, doi: 10.1016/j.canlet.2011.10.001, indexed in Pubmed: 22050907.
23. Pothuraju R, Rachagani S, Krishn SR, et al. Molecular implications of MUC5AC-CD44 axis in colorectal cancer progression and chemoresistance. Mol Cancer. 2020; 19(1): 37, doi: 10.1186/s12943-020-01156-y, indexed in Pubmed: 32098629.
24. Li M, Wan G, Yu H, et al. High-intensity focused ultrasound inhibits invasion and metastasis of colon cancer cells by enhancing microRNA-124-mediated suppression of STAT3. FEBS Open Bio. 2019; 9(6): 1128–1136, doi: 10.1002/2211-5463.12642, indexed in Pubmed: 30980700.
25. Manzotti C, Audisio RA, Pratesi G. Importance of orthotopic implantation for human tumors as model systems: relevance to metastasis and invasion. Clin Exp Metastasis. 1993; 11(1): 5–14, doi: 10.1007/BF00880061, indexed in Pubmed: 8422706.
26. Madersbacher S, Pedevilla M, Vingers L. Effect of high-intensity focused ultrasound on human prostate cancer in vivo. Cancer Res. 1995; 55(15): 3346–3351, indexed in Pubmed: 7542168.
27. Hectors SJ, Jacobs I, Moonen CTW, et al. MRI methods for the evaluation of high intensity focused ultrasound tumor treatment: Current status and future needs. Magn Reson Med. 2016; 75(1): 302–317, doi: 10.1002/mrm.25758, indexed in Pubmed: 26096859.
28. Lee YY, Cho YJ, Choi JJ, et al. The effect of high-intensity focused ultrasound in combination with cisplatin using a Xenograft model of cervical cancer. Anticancer Res. 2012; 32(12): 5285–5289, indexed in Pubmed: 23225428.
29. Zhong J, Bambrook J, Bhambra B, et al. Incidence of post-ablation syndrome following image-guided percutaneous cryoablation of renal cell carcinoma: a prospective study. Cardiovasc Intervent Radiol. 2018; 41(2): 270–276, doi: 10.1007/s00270-017-1811-1, indexed in Pubmed: 29185017.
30. Chu KF, Dupuy DE. Thermal ablation of tumours: biological mechanisms and advances in therapy. Nat Rev Cancer. 2014; 14(3): 199–208, doi: 10.1038/nrc3672, indexed in Pubmed: 24561446.
31. Tonguc T, Strunk H, Gonzalez-Carmona MA, et al. US--guided high-intensity focused ultrasound (HIFU) of abdominal tumors: outcome, early ablation-related laboratory changes and inflammatory reaction. A single-center experience from Germany. Int J Hyperthermia. 2021; 38(2): 65–74, doi: 10.1080/02656736.2021.1900926, indexed in Pubmed: 34420445.
32. Ektate K, Munteanu MC, Ashar H, et al. Chemo-immunotherapy of colon cancer with focused ultrasound and Salmonella-laden temperature sensitive liposomes (thermobots). Sci Rep. 2018; 8(1): 13062, doi: 10.1038/s41598-018-30106-4, indexed in Pubmed: 30166607.
33. Maeda M, Muragaki Y, Okamoto J, et al. Sonodynamic therapy based on combined use of low dose administration of epirubicin-incorporating drug delivery system and focused ultrasound. Ultrasound Med Biol. 2017; 43(10): 2295–2301, doi: 10.1016/j.ultrasmedbio.2017.06.003, indexed in Pubmed: 28705555.
34. Wu Y, Zhang J, Yu S, et al. Cell pyroptosis in health and inflammatory diseases. Cell Death Discov. 2022; 8(1): 191, doi: 10.1038/s41420-022-00998-3, indexed in Pubmed: 35411030.
35. Wallach D, Kang TB, Kovalenko A. Concepts of tissue injury and cell death in inflammation: a historical perspective. Nat Rev Immunol. 2014; 14(1): 51–59, doi: 10.1038/nri3561, indexed in Pubmed: 24336099.
36. Cutts SM, Swift LP, Rephaeli A. Sequence specificity of adriamycin-DNA adducts in human tumor cells. Mol Cancer Ther. 2003; 2(7): 661–670, indexed in Pubmed: 12883039.
37. Karki R, Man SiM, Kanneganti TD. Inflammasomes and Cancer. Cancer Immunol Res. 2017; 5(2): 94–99, doi: 10.1158/2326-6066.CIR-16-0269, indexed in Pubmed: 28093447.
38. Allen IC, TeKippe EM, Woodford RMT, et al. The NLRP3 inflammasome functions as a negative regulator of tumorigenesis during colitis-associated cancer. J Exp Med. 2010; 207(5): 1045–1056, doi: 10.1084/jem.20100050, indexed in Pubmed: 20385749.
39. Biermann K, Montironi R, Lopez-Beltran A, et al. Histopathological findings after treatment of prostate cancer using high-intensity focused ultrasound (HIFU). Prostate. 2010; 70(11): 1196–1200, doi: 10.1002/pros.21154, indexed in Pubmed: 20564422.
40. Hsiao YH, Kuo SJ, Tsai HD, et al. Clinical application of high-intensity focused ultrasound in cancer therapy. J Cancer. 2016; 7(3): 225–231, doi: 10.7150/jca.13906, indexed in Pubmed: 26918034.
41. Furusawa Y, Hassan MA, Zhao QL, et al. Effects of therapeutic ultrasound on the nucleus and genomic DNA. Ultrason Sonochem. 2014; 21(6): 2061–2068, doi: 10.1016/j.ultsonch.2014.02.028, indexed in Pubmed: 24657073.
42. Rix A, Lederle W, Theek B, et al. Advanced ultrasound technologies for diagnosis and therapy. J Nucl Med. 2018; 59(5): 740–746, doi: 10.2967/jnumed.117.200030, indexed in Pubmed: 29496981.
43. Mouratidis PXE, Ter Haar G. Latest advances in the use of therapeutic focused ultrasound in the treatment of pancreatic cancer. Cancers (Basel). 2022; 14(3), doi: 10.3390/cancers14030638, indexed in Pubmed: 35158903.

Submitted: 13 September, 2022
Accepted after reviews: 24 January, 2023
Available as AoP: 20 February, 2023